Energy Conversion and Management 78 (2014) 518–526

Contents lists available at ScienceDirect

Energy Conversion and Management

journal homepage: www.elsevier.com/locate/enconman

Pyrolysis of *Jatropha curcas* pressed cake for bio-oil production in a fixed-bed system

Seyed Amirmostafa Jourabchi [a], Suyin Gan [a,*], Hoon Kiat Ng [b]

[a] Department of Chemical and Environmental Engineering, The University of Nottingham Malaysia Campus, Jalan Broga, 43500 Semenyih, Selangor Darul Ehsan, Malaysia
[b] Department of Mechanical, Materials and Manufacturing Engineering, The University of Nottingham Malaysia Campus, Jalan Broga, 43500 Semenyih, Selangor Darul Ehsan, Malaysia

ARTICLE INFO

Article history:
Received 7 August 2013
Accepted 8 November 2013
Available online 8 December 2013

Keywords:
Pyrolysis
Jatropha curcas
Bio-oil
Optimisation
Empirical correlation

ABSTRACT

This study investigated the effects of pyrolysis parameters on the yield and quality of bio-oil from *Jatropha curcas* pressed cake. This biomass was pyrolysed in a fixed-bed reactor over a temperature range of 573.15 K to 1073.15 K and a nitrogen linear speed range of 7.8×10^{-5} m/s to 6.7×10^{-2} m/s. The heating rate and biomass grain size were 50 K/min and <2 mm, respectively. The bio-oils were tested for the gross calorific value, water content and acidity. The pyrolysis process was simulated using Thermo-Gravimetric Analysis (TGA) and Differential Scanning Calorimeter (DSC) for mass and energy balances analyses. Empirical correlations between the bio-oil specifications and pyrolysis parameters were developed using linear and nonlinear multiple regression methods for process optimisation. At optimum pyrolysis conditions, above 50% of the waste is converted to bio-oil with less than 30% water content, a gross calorific value of 15.12 MJ/kg and a pH of 6.77.

1. Introduction

Biomass based on its availability and its status as a waste product is a prime source of renewable energy worldwide. Amongst the many varied ways to utilise biomass as a source of energy is pyrolysis, a thermochemical decomposition process that occurs at elevated temperatures in the absence of oxygen gas. Biomass pyrolysis produces gas and liquid products, and leaves a solid residue known as char [1]. The liquid product is a fuel termed as bio-oil, pyrolysis oil or bio-crude [2]. Presently, bio-oil produced from the pyrolysis of biomass can be used directly or after further physicochemical processes to heat up boilers, or even drive diesel engines or turbines [3–5]. It can be stored and transported more efficiently compared to the original biomass because of its liquid state. During the combustion of bio-oil, its net zero carbon dioxide (CO_2) as well as lesser nitrogen oxides (NO_x) and/or sulphur oxides (SO_x) emissions compared to fossil fuels makes it a potential liquid fuel replacement [6].

In this study, the feedstock of interest is *Jatropha curcas (J. curcas)*, a drought-free and inedible crop, which can be planted economically in tropical and sub-tropical regions [7]. Its seed is a source of oil that is used currently for commercial biodiesel production. Nevertheless, the extraction of oil for the purpose of biodiesel production only takes up to 18 wt% of the dry fruit, but it has been reported that the remaining *J. curcas* fruit after biodiesel production has the potential of fuel production with twice the energy content compared to biodiesel [8]. Different parts of the *J. curcas* shrub can be utilised in a number of thermochemical processes. Vyas and Singh [9], for example, showed that *J. curcas* seed husk could successfully be used as feedstock for open core down draft gasifier to generate producer gas. For pyrolysis, approximately 50 wt% of its nutshell can be transformed into bio-oil and even its wood and leaves can be valorised for fuel extraction [10]. The pressed cake remaining after oil extraction can also be used as a source of bio-oil production as reported by Sricharoenchaikul and Atong [11]. In their work, Thermo-Gravimetric Analysis (TGA) and a fixed-bed quartz reactor were used to determine a suitable degradation model and investigate the effect of operating conditions on product distribution. It was found that the main thermal decomposition occurred over the temperature range of 523.15–723.15 K and could be described by the three-parallel reactions model. The temperature and hold time within the fixed-bed quartz reactor influenced the yields of gas, liquid and char products although full optimisation was not carried out here. Similarly, Antony Raja et al. [12] carried out a parametric study of flash pyrolysis of *Jatropha* oil cake in an electrically heated fluidised bed reactor using nitrogen (N_2). Maximum oil yield of 64.25 wt% was obtained at a particle size of 1.0 mm, a pyrolysis temperature of 773.15 K and a N_2 gas flow rate of 1.75 m^3/h. The obtained pyrolysis oil had a calorific value of 19.66 MJ/kg and could be used as a source of low-grade fuel directly or upgraded to a higher quality bio-fuel.

To date, while a number of research studies have indicated the potential of *J. curcas* wastes as pyrolysis feedstock, only the effect

* Corresponding author. Tel.: +60 3 8924 8162; fax: +60 3 8924 8017.
E-mail address: suyin.gan@nottingham.edu.my (S. Gan).

0196-8904/$ - see front matter © 2013 Elsevier Ltd. All rights reserved.
http://dx.doi.org/10.1016/j.enconman.2013.11.005

of temperature on the bio-oil yield has been reported on laboratory-scale fixed-bed reactor setups [11]. Full optimisation of pyrolysis parameters to maximise not only *J. curcas* bio-oil yield, but also its quality has yet to be carried out. Therefore, the focus of this study is to ascertain the effects of pyrolysis parameters on the yield and quality of bio-oil as well as to determine the operating conditions required to obtain optimum quantity and quality of bio-oil from *J. curcas* pressed cake. To achieve this, a laboratory-scale fixed-bed pyrolysis reactor and a condenser were designed and fabricated which allowed slow pyrolysis experiments to be conducted. Under this setting, the two key parameters investigated in this study were temperature and N_2 linear speed. Design of Experiment (DoE) was performed along with linear and nonlinear multiple regression methods in order to determine the optimum pyrolysis parameters.

2. Methodology

2.1. Biomass feedstock

J. curcas pressed cake waste was obtained from Bionas Group (Malaysia) to be used as the pyrolysis feedstock. This waste was prepared for the pyrolysis tests by grinding it into powder form in a 2-step process. Firstly, the pressed cake was converted into granules using a Retsch SM100 Comfort grinder machine. Secondly, the granules were ground and sieved using a sieve size of 0.2 mm in a Retsch ZM200 centrifuge grinder.

Characterisation tests were carried out on the *J. curcas* pressed cake. TGA was carried out on the *J. curcas* pressed cake to determine its moisture, volatiles, fixed carbon and ash contents on a Mettler-Toledo TGA/DSC 1 unit following the method described by Sluiter et al. [13]. The moisture content was also determined via the oven drying method based on the American Society for Testing and Materials (ASTM) D4442-07 method. The gross calorific value of the biomass was measured by using a Parr 6100 calorimetric bomb based on the ASTM D2015-96 method. Thermo Conductivity Detector Infra Red (TCD-IR) was used to analyse the organic elements (C–H–N–O). As for inorganic elements, the milled *J. curcas* waste was analysed by using Inductively Coupled Plasma Mass Spectrometry (ICP-MS) Thermo-Fisher Scientific X-Series^{II} equipped with Collision Cell Technology with Energy Discrimination (CCTED). For the rest of detectable elements not measured by the ICP-MS, Energy Dispersive X-ray Spectroscopy (EDX) Oxford Instrument Analytical model X-Max Silicon Drift Detector 20 mm^2 was used. ^{13}C Nuclear Magnetic Resonance (NMR) was utilised to determine the fraction of organic compounds in the biomass. With the exception of TGA, calorific value and EDX which were carried out using in-house analytical facilities, all other characterisation tests were carried out at the University of Nottingham, United Kingdom.

2.2. Pyrolysis rig

Fig. 1(a) and (b) show the schematic diagram of the pyrolysis process and the configurations of the reactor and condenser, respectively. The design of the fixed-bed pyrolysis rig was carried out using Pro/Engineering Wildfire 3.0 software and the rig was mainly fabricated in the University of Nottingham Malaysia Campus workshops. The material of construction was chosen as stainless steel since the rig was designed to withstand a maximum temperature of 1073.15 K in addition to predicted acidic conditions due to the bio-oil product [14]. Stainless steel has a high melting point and is resistant to chemical reactions and acidic conditions [14]. Additionally, its high strength renders it a long lasting material of choice for pyrolysis systems. The only drawback of using stainless steel in the fabrication of the rig was that welding was not as easy as compared to other iron-based materials. This problem was solved by using Tungsten Inert Gas (TIG) welding to yield a smooth surface with no leaking joints. To prevent leakages from detachable joints, brass and copper plates were used as gasket and washer, respectively. The unavoidable use of these two metals limited the maximum reaction temperature to 1073.15 K to prevent any melt down of these sealing materials.

The detachable fixed bed reactor has an inner diameter of 52.502 mm connected to a shell and tube condenser to quench the released volatiles. By matching the reactor geometry, a Carbolite tubular furnace type CTF 12/65/550 with a maximum heating rate of 50 K/min is used as a heater. Preliminary investigations showed that significant uneven heat distribution along the tubular furnace existed. Using reactors equal to or longer than the length of furnace resulted in re-condensation of volatiles inside the reactor. This phenomenon was the main factor that prevented proper bio-oil collection as the volatiles condensed and covered the inner wall of the reactor only. Therefore, the length of the reactor was selected to be equal to the maximum heating zone inside the tubular furnace to overcome the above-mentioned problem (Fig. 1(b)). Preliminary experimental observations also indicated that it was possible under certain conditions for the biomass to be transformed directly into liquid bio-oil within the reactor. Both the placement of the reactor outlet tube at the minimum height position and inclining the reactor at a 20° angle from the horizontal ensured the collection of this portion of bio-oil. Low-pressure N_2 and gravitational force were used in the whole process to forward both the gas and liquid along the rig. The slanted tube then bends into the vertical condenser to allow gravitational force to drive the bio-oil into the collector at the bottom (Fig. 1(b)).

The condenser utilises cooling water in a counter-current flow arrangement from a refrigerated bath circulator type 632D. The heat transfer area of the condenser was designed such that the outlet gas temperature is below 303.15 K when the cooling water temperature is fixed at 278.15 K. The vertical orientation of the condenser also improved the convection heat transfer as gas with higher energy and temperature tends to rise up while cooler gas is forced down via natural convection. The inner tube of the condenser was milled to firstly, reduce the wall thickness and secondly, to create a finned tube to maximise the heat transfer surface area between the water and the gaseous volatiles.

2.3. Design of Experiment (DoE)

The biomass was pyrolysed over a temperature range of 573.15 K to 1073.15 K and a N_2 linear speed range of 7.8×10^{-5} m/s to 6.7×10^{-2} m/s to produce bio-oil in a full factorial matrix as listed in Table 1. Preliminary tests showed that at temperatures below 573.15 K, no tangible reactions were occurring in the reactor hence this limited the minimum reaction temperature. The N_2 velocity was initially set to three different values with a minimum velocity of 0.7×10^{-2} m/s and increments of 3 m/s, but after observing that low N_2 velocity positively impacted the bio-oil yield, the tested range was expanded to five values with a minimum velocity of 7.8×10^{-5} m/s chosen based on the flow meter limitation. The heating rate was fixed to a constant of 50 K/min corresponding to the maximum possible setting on the furnace. In this study, the biomass grain size was fixed to be <0.2 mm as a commonly used medium particle size in the literature in addition to the availability of a matching sieve size [15–17]. Furthermore, Pütün et al. [18] reported that the effect of biomass grain size on bio-oil production was negligible. For consistency, 50 ± 1 g samples were used in all test runs and the tests were repeated three times. The holding time for the completion of each test as indicated by no visible outlet gas and/or bio-oil droplets in the collector depended on the pyrolysis conditions. The minimum holding time recorded was 30 min and the

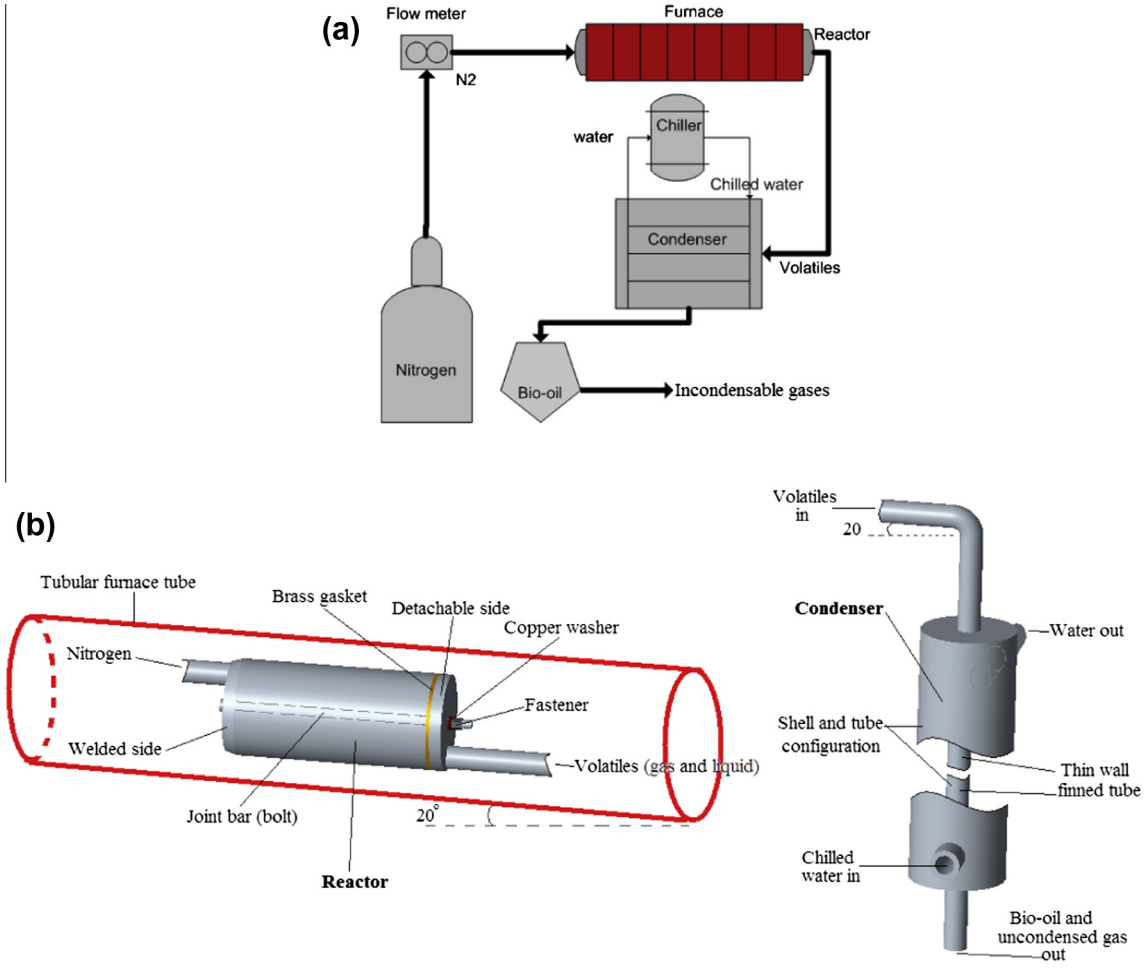

Fig. 1. Pyrolysis rig: (a) schematic diagram of the process and (b) reactor and condenser configurations.

Table 1
Design of Experiment (DoE) for pyrolysis tests.

Pyrolysis parameters	Unit	Min	Max	Increment	Variations
Reaction temperature	K	573.15	1073.15	125	5
Nitrogen linear speed	cm/s	0.0078	6.7	0.6922 and 3	5
Biomass grain size	mm	0.2		–	1
Condenser temperature	K	278.15		–	1
Holding time	min	maximum 90		–	1
Repeatability					3
total number of experimental runs					75

maximum was 90 min. For all test runs, the masses of the collected bio-oil comprising both the light and heavy phases, as well as the remaining char were measured to determine their yields.

2.4. Analytical tests

Every bio-oil sample was subjected to analytical testing of three important bio-oil specifications, i.e. gross calorific value, water content and acidity. As stated earlier, the bio-oil samples collected comprised two phases, i.e. a light phase and a heavy phase. The analytical tests were carried out after homogenising the bio-oil sample to create a temporary single-phase suspension mixture. This ensured that the tests were conducted on the mixture of both light and heavy phases. Each analytical test was carried out at least twice or more for consistent results with repeatability within 5% error.

2.4.1. Heat of combustion

The gross calorific value of the bio-oil products were tested according to the ASTM D240 method using a Parr 6100 calorimetric bomb unit. Based on the fact that bio-oil contains considerable water content thereby preventing proper ignition in the calorimetric bomb unit, cotton was used to prevent any misfire in the process [19–20]. The bio-oil and cotton were individually weighed before each test to determine the heat of combustion of pure bio-oil.

2.4.2. Water content

The ASTM E203 method was used in the measurement of water content using a Mettler Toledo V20 Karl Fischer titrator unit. Based on preliminary testing results, methanol could not be used as a solvent in the Karl Fischer titrator because of its reaction with ketones producing water as a result [19–20]. To prevent this reaction, the Combisolvent Keto (Merck) was used in replacement of methanol.

Accordingly, the CombiTitrant 5 Keto (Merck) was also used to give accurate water content results. To ensure consistency in results, a weight ratio of 9:1 of bio-oil and solvent, respectively was used for every bio-oil sample.

2.4.3. Acidity

The ASTM E70 method was adhered to when measuring the pH of the bio-oil samples by using a Metrohm 785 DMP Titrino auto titrator unit. To ensure repeatable results, the samples were continuously stirred to obtain homogeneous samples while the pH readings were recorded.

2.4.4. Thermo-Gravimetric Analysis (TGA) and Differential Scanning Calorimeter (DSC)

Although mass measurements and analytical tests of the bio-oil product can provide a comprehensive picture of the effects of pyrolysis parameters on bio-oil quantity and quality, fundamental knowledge of the heat and mass transfer occurring inside the reactor is limited. Both TGA and DSC analyses enable a better understanding of the physical and chemical reactions that are taking place inside the pyrolysis reactor.

Each experimental test point was also tested by using a Mettler-Toledo TGA/DSC 1 unit to simulate the heat and mass transfer of the actual experiment. This was accomplished by downsizing the actual experimental geometry into the size of the TGA/DSC unit. The geometry of the TGA/DSC unit was measured and the actual experiments were simulated in such a way that the N_2 linear speed was the same as the actual experiments.

3. Results and discussion

3.1. Physicochemical properties of J. curcas waste

Table 2 summarises the physicochemical properties that were measured for the *J. curcas* pressed cake. The TGA shows that the *J. curcas* pressed cake contains less than 4 wt% moisture and over 70 wt% volatiles, both of which are indicative of the potential bio-oil content. The analysis also shows that 70% of the total volatiles separation occurs at temperatures below 650 K, which is relatively low and hence aids in reducing the energy consumption during the pyrolysis process. The amount of moisture content both from the TGA and from the oven drying method have matching results of below 4 wt%. This is relatively low considering that under Malaysian climate condition, the average humidity is approximately 80% [21]. By having a moisture content below 10%, the drying process can be skipped completely before pyrolysis which is an advantage of this biomass source since energy is saved for the total bio-oil production process [4]. Comparatively high gross calorific value, high carbon and volatiles content, low nitrogen and elementals content, as well as similar oxygen content to other biomass sources indicate the potential of *J. curcas* pressed cake as a source of bio-fuel.

Bio-oil is a complex mixture of many organic compounds whose composition depends on the cellulose, hemicellulose and lignin contents in the biomass. Acids, aldehydes, alcohols and ketones are the products of cellulose and hemicelluloses while phenolics and cyclic oxygenates are the products of lignin [22]. As can be seen in Table 2, the high cellulose content in *J. curcas* pressed cake is predicted to produce a large amount of alcohols in addition to unfavourable ketones and aldehydes in the bio-oil product. However, this can be compensated by the low lignin content which reduces the amount of phenolic and cyclic oxygenates in the bio-oil.

3.2. Bio-oil yield

Fig. 2 shows how the N_2 velocity and reaction temperature affect the bio-oil yield as well as the key specifications of the bio-oil product. The key specifications include water content, gross calorific value and acidity, all of which were measured at least twice for each bio-oil sample. For each test point, three samples were collected hence a minimum of six measurements were made. The average measurements are plotted in Fig. 2. The error bars shown indicate the maximum and minimum values for each test point. In Fig. 2(a), it is clearly shown that the bio-oil yield obtained from the

Table 2
Physicochemical properties of *Jatropha curcas* pressed cake.

Property	Unit	Value	Method
Moisture content	wt%	3.40	Oven drying
Gross calorific value	MJ/kg	19.11	Bomb calorimeter
Moisture content	wt%	3.31	Thermo-gravimetric analysis
Volatiles content		70.98	
Fixed carbon content		19.72	
Ash content		5.99	
Carbon (C)	wt%	45.75	Thermo conductivity detector infra red
Oxygen (O)		38.20	
Hydrogen (H)		6.24	
Nitrogen (N)		3.56	
Potassium (K)	wt%	1.87	Inductively coupled plasma mass spectrometry
Magnesium (Mg)		0.79	
Calcium (Ca)		0.52	
Iron (Fe)		0.10	
Sodium (Na)		0.05	
Aluminium (Al)		0.02	
Phosphorus (P)	wt%	0.75	Energy dispersive X-ray spectroscopy
Sulphur (S)		0.22	
Silicon (Si)		0.09	
Undetectable elements	wt%	1.84	By calculation
Cellulose	Carbon wt%	48.92	^{13}C Nuclear Magnetic Resonance
Lignin		25.00	
Hemicellulose		13.04	
Cellulose C1		6.52	
Aliphatic		6.52	

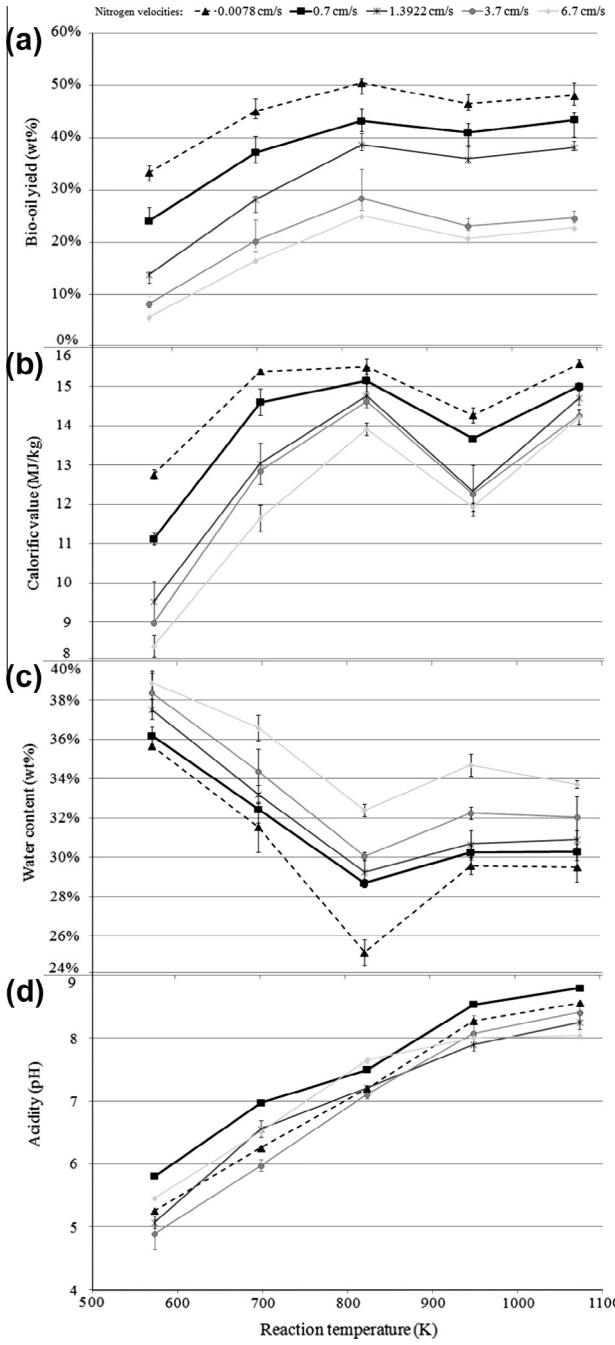

Fig. 2. Effect of temperature and N_2 velocity on bio-oil (a) yield, (b) calorific value, (c) water content and (d) acidity.

fixed-bed pyrolysis rig increases when the velocity of N_2 flowing through the bed reduces. The phenomenon is likely to be caused by the unnecessary cooling effect of extra N_2 in the bed at higher linear speeds. The N_2 flowing through the bed should only be enough to ensure that no O_2 is available in the bed for reactions to occur with the heated biomass. The unnecessary cooling in the bed due to the extra N_2 prevents uniform heating of the biomass and consequently, limits the necessary cracking of the biomass. This delay in cracking and bonding prolongs the duration of the pyrolysis process as observed during the experiments which is unfavourable from the aspect of energy consumption. Fig. 2(a) also shows that for a fixed N_2 flow rate and hence velocity, when the reaction temperature increases, the bio-oil yield increases to a maximum amount at approximately 823.15 K. Above this temperature, a slight decrease

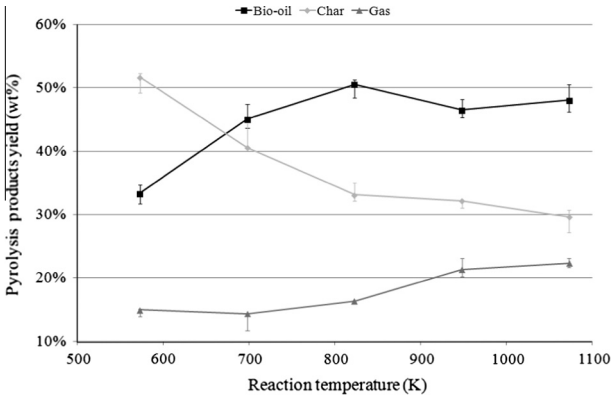

Fig. 3. Pyrolysis products against reaction temperature for a N_2 velocity of 0.0078 cm/s.

is experienced followed by a final increase. The slow heating rate of the furnace, i.e. 50 K/min implies that the biomass experiences a longer residence time from 573.15 up till 823.15 K. This means that by having a higher heating rate, the final reaction temperature for maximum bio-oil yield might be reduced.

Fig. 3 illustrates the yields of bio-oil and its two by-products, i.e. char and gas at the minimum N_2 velocity of 0.0078 cm/s, which corresponds to maximum bio-oil yield seen in Fig. 2(a). At temperatures below 573.15 K, no noticeable bio-oil product is observed because the heat is sufficient to crack the hemicellulose only and produce mainly carbon monoxide (CO) and CO_2 gases [6]. Within the temperature range of 623.15 K to 773.15 K, the cellulose first breaks down, and then the lignin starts to crack down into char, water and heavy oil [6]. This justifies the decrease in char production in favour of higher bio-oil product and almost constant amount of gas shown in Fig. 3. It also shows that beyond 823.15 K, further gasification occurs (rise in gas curve in Fig. 3), and fine and light gases such as H_2 are generated (that cannot be trapped in condenser) resulting in lower bio-oil production compared to lower temperature [6].

3.3. Bio-oil characterisation

3.3.1. Heat of combustion

Fig. 2(b) shows gross calorific values of the bio-oils produced at all test points. The chemical compositions of the bio-oil samples produced under different test conditions are different as the reactions occurring in the bed are dependent on both N_2 velocity and temperature. Consequently, the heat of combustion is not expected to be the same for all samples.

Additionally, the amount of water content in the bio-oil has a direct effect on the gross calorific value. Fig. 2(b) and (c) depict that the gross calorific value and water content curves are horizontally symmetrical which indicate that the major factor affecting the heat of combustion is the water content in the bio-oil. The ASTM specification for gross calorific value of pyrolysis liquid bio-fuels to be used in burners is a minimum of 15 MJ/kg [23]. Not only do the unprocessed bio-oils meet this specification between the temperatures of 670 K and 850 K for lower N_2 linear speed test points, but the calculated gross calorific values of dry bio-oils for the same region are approximately 20 MJ/kg, which is above the ASTM D7544-10 requirement for burner fuels.

3.3.2. Water content

Fig. 2(c) shows that the percentage of water content in the produced bio-oil samples is maximum at the lowest temperature of 573.15 K and continues to decrease with increase in temperature

until a minimum is obtained at approximately 823.15 K. Thereafter, the water content increases to a limited maximum point depending on the N_2 flow rate. The horizontally symmetrical curves in Fig. 2(a) and Fig. 2(c) suggest that at a temperature of approximately 823.15 K, not only cracking and bonding are maximised, but they are also optimised in producing more oil and heavy oil in the bio-oil product with less water. Fig. 2(c) also indicates that by increasing the N_2 speed, unnecessary cooling in bed occurs and consequently, this disturbs the cracking process leading to increased water content in the bio-oil. The maximum allowable water content in liquid bio-fuels is limited to 30 wt% according to ASTM D7544-10 [23]. The tested bio-oil samples that which meet this limit are those produced at reaction temperatures above 730 K and at minimum N_2 linear speed.

3.3.3. Acidity of bio-oil

One of the drawbacks of bio-oil is its typical acidity condition [4]. The results of the ASTM E70 test method on the *J. curcas* bio-oil samples show that the pH values range from 4.9 to 8.8 as depicted in Fig. 2(d). It is clear from Fig. 2(d) that as temperature increases, the pH increases while the N_2 linear speed does not appear to affect the pH as much. The results indicate that the chemical composition of bio-oil is more highly dependent on reaction temperature than N_2 linear speed. Furthermore, it can be seen that at temperatures approximately 800 K, all the tests showed pH values close to 7, which can be considered as neutral.

3.4. Empirical correlations

First, by averaging the triplicate test results for bio-oil yield, a total number of 25 test points have been used to develop an empirical correlation for bio-oil yield. By using nonlinear multiple regression method, the relationship between the experimental variable and bio-oil yield can be modelled [24]. For each test, there are two variables of reaction temperature and N_2 linear speed in the bed. By looking at Fig. 2(a), the partial correlation between reaction temperature and bio-oil yield can be modelled as a cubic polynomial. On the other hand, the partial correlation between N_2 linear speed in the bed and bio-oil yield can be modelled as a quadratic polynomial. Generalising these partial correlations into a multiple correlation by summation of the two aforementioned polynomials, the following equation can be written:

$$B = c + n_1 N + n_2 N^2 + t_1 T + t_2 T^2 + t_3 T^3 \quad (1)$$

In Eq. (1), B, N and T are the bio-oil yield, N_2 linear speed and reaction temperature, respectively. To find the constant number c and the other five coefficients, six equations need to be defined and solved simultaneously. As Eq. (1) is valid over the range of experimental matrix, all test points can be described by it. Likewise, the summation of all the experimental points can be described by Eq. (2):

$$\sum B_i = c + n_1 \sum N_i + n_2 \sum N_i^2 + t_1 \sum T_i + t_2 \sum T_i^2 + t_3 \times \sum T_i^3 \quad (2)$$

By multiplying Eq. (1) by different powers of N and T or a combination of both, and using the summation in Eq. (2), the five equations below can be generated:

$$\sum N_i B_i = c \sum N_i + n_1 \sum N_i^2 + n_2 \sum N_i^3 + t_1 \sum N_i \cdot T_i + t_2 \sum N_i \cdot T_i^2 + t_3 \sum N_i \cdot T_i^3 \quad (3)$$

$$\sum T_i \cdot N_i \cdot B_i = c \sum T_i \cdot N_i + n_1 \sum T_i \cdot N_i^2 + n_2 \sum T_i \cdot N_i^3 + t_1 \sum T_i^2 \cdot N_i + t_2 \sum T_i^3 \cdot N_i + t_3 \sum T_i^4 \cdot N_i \quad (4)$$

$$\sum T_i \cdot N_i^2 \cdot B_i = c \sum T_i \cdot N_i^2 + n_1 \sum T_i \cdot N_i^3 + n_2 \sum T_i \cdot N_i^4 + t_1 \sum T_i^2 \cdot N_i^2 + t_2 \sum T_i^3 \cdot N_i^2 + t_3 \sum T_i^4 \cdot N_i^2 \quad (5)$$

$$\sum T_i^2 \cdot N_i^2 \cdot B_i = c \sum T_i^2 \cdot N_i^2 + n_1 \sum T_i^2 \cdot N_i^3 + n_2 \sum T_i^2 \cdot N_i^4 + t_1 \sum T_i^3 \cdot N_i^2 + t_2 \sum T_i^3 \cdot N_i^2 + t_3 \sum T_i^5 \cdot N_i^2 \quad (6)$$

$$\sum T_i^3 \cdot N_i^2 \cdot B_i = c \sum T_i^3 \cdot N_i^2 + n_1 \sum T_i^3 \cdot N_i^3 + n_2 \sum T_i^3 \cdot N_i^4 + t_1 \sum T_i^4 \cdot N_i^2 + t_2 \sum T_i^5 \cdot N_i^2 + t_3 \sum T_i^6 \cdot N_i^2 \quad (7)$$

The constants of Eq. (1) can be found by solving the above 6 by 6 simultaneous equations (Eqs. (2)–(7)) to result in Eq. (8) below where B is in wt%, N is in cm/s and T is in K/1000:

$$B = -58.31 - 9.95\,N + 0.95\,N^2 + 176.98\,T + 0.01\,T^2 - 68.8599\,T^3 \quad (8)$$

Similarly, by using the same method, the quality specifications of bio-oil can be modelled by relating them to the pyrolysis parameters (for acidity only, linear multiple regression method is used instead of nonlinear). The results for gross calorific value (C in MJ/kg), water content (W in wt%) and acidity (P in pH scale) are shown by Eqs. (9)–(11), respectively where similarly, for all of them, N is in cm/s and T is in K/1000:

$$C = 1.46 - 0.97\,N + 0.09\,N^2 + 20.11\,T - 0.002\,T^2 - 5.48\,T^3 \quad (9)$$

$$W = 73.57 + 0.68\,N - 96.86\,T + 52.27\,T^2 \quad (10)$$

$$P = 1.97 - 0.03\,N + 6.36\,T \quad (11)$$

To validate the above models, first, the results from the proposed correlations are compared to the experimental results and over the experimental range tested, the maximum error is below

Table 3
Validation of empirical correlations.

Points	Unit		1	2	3	4	Opt.[a]	Max.[a] error (%)
Reaction temperature	K		636.15	761.15	886.15	1011.15	800.17	
N_2 linear velocity	cm/s		0.351	5.1948	1.0452	2.5428	0.0078	
Bio-oil yield	wt%	Exp.[a]	33.69	19.58	41.57	31.31	50.08	4.25
		Emp.[a]	33.18	19.89	41.24	30.28	47.95	
Gross calorific value	MJ/kg	Exp.	12.77	12.17	14.14	14.43	15.12	3.19
		Emp.	12.51	11.78	14.55	14.25	14.74	
Water content	wt%	Exp.	32.34	35.26	28.64	29.28	28.34	4.59
		Emp.	33.34	33.64	29.49	30.79	29.54	
Acidity	pH	Exp.	6.01	6.52	7.58	8.74	6.77	4.66
		Emp.	6.00	6.67	7.57	8.33	7.05	

[a] Exp.: experimental; Emp.: empirical; Opt.: optimum; Max.: maximum.

5%. The second validation step is to choose four previously untested points for pyrolysis testing (in between the original test points) and compare the test results with the modelling results to ensure that the error is below 5% for all of them. Table 3 summarises the validation results, which are all below 5% error.

Since the models were obtained from a full factorial test set (DoE) and validated experimentally, they can be used to predict the behaviour of the pyrolysis process under any experimental conditions (variables) as long as the conditions are within the test matrix range.

3.5. Optimisation

Although the experimental results can directly give the optimum experimental point for each individual specification of bio-oil (e.g. gross calorific value), from a practical viewpoint, it would be necessary to determine the optimum point for best combined yield and quality specifications. The optimum point is not necessarily one of the experimental points and is found by using the developed empirical correlations.

Normalisation is used to combine the effects of pyrolysis parameters on bio-oil yield and quality specifications. B_1, C_1, W_1 and P_1 (P_1 is pH closest to 7) are the optimum bio-oil yield, gross calorific value, water content and pH of bio-oil, respectively whereas B_2, C_2, W_2 and P_2 are their worst counterparts. Four dimensionless numbers (b, c, w and p) are defined for the four specifications of interest:

$$b = \frac{B - B_2}{B_1 - B_2} \Rightarrow 0 \leqslant b \leqslant 1 \tag{12}$$

$$c = \frac{C - C_2}{C_1 - C_2} \Rightarrow 0 \leqslant c \leqslant 1 \tag{13}$$

$$w = 1 - \frac{W - W_1}{W_2 - W_1} \Rightarrow 0 \leqslant w \leqslant 1 \tag{14}$$

$$p = 1 - \frac{|P - 7| - |P_1 - 7|}{|P_2 - 7| - |P_1 - 7|} \Rightarrow 0 \leqslant p \leqslant 1 \tag{15}$$

For each specification, the empirical correlations are used to generate a comprehensive data set by setting the resolutions of the N_2 flow meter and tubular furnace thermometer as the increments within the iteration loops. A computer programme is written using Matlab software for this purpose. By iterating for each point, dimensionless numbers can be found for each individual bio-oil specification. 0 represents the worst point while 1 represents the optimum point for each individual specification. The average (index number i) of all four numbers is a number between 0 and 1:

$$i = \frac{b + c + w + p}{4} \Rightarrow 0 \leqslant i \leqslant 1 \tag{16}$$

The maximum amount of this number (closest to one) represents the optimum point considering all four combined specifications. An experimental pyrolysis test was finally carried out under the optimum conditions. A comparison of both experimental and modelling results as listed in Table 3 shows that the error is below 5%. This, in addition to the validation described in Section 3.4, demonstrates the validity of the developed empirical correlations as well as the proposed optimisation process.

The validated model shows that optimum combined quantity and quality of bio-oil occurs at a reaction temperature of 800.17 K and a N_2 linear speed of 0.0078 cm/s (Table 3). The experimental results shows that at this point, 50.08 wt% of *J. curcas* pressed cake is converted to bio-oil with a gross calorific value of 15.12 MJ/kg, water content of 28.34 wt% and pH of 6.77 (Table 3).

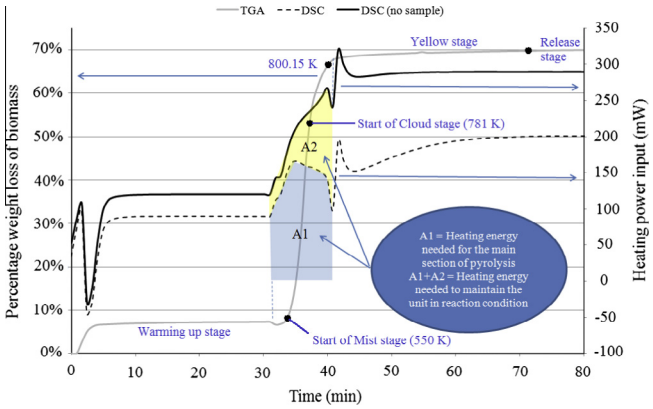

Fig. 4. Heat and mass transfer characteristics during the pyrolysis process at optimum point.

3.6. Thermo-Gravimetric Analysis (TGA) and Differential Scanning Calorimeter (DSC)

Fig. 4 illustrates the heat and mass transfer characteristics of the pyrolysis process using the combined results of both TGA and DSC. The analysis was conducted under optimum pyrolysis conditions for best combined quantity (yield) and quality of bio-oil. In Fig. 4, the weight loss of biomass in the bed (TGA curve with solid grey line) and the heating power required for pyrolysis process (DSC curve with dashed black line) are plotted. For the purpose of energy calculations, the heating power curve (DSC curve with solid black line) is also plotted for the period that the unit was run without any biomass inside. By interpreting the data shown in both Figs. 3 and 4 in addition to recorded experimental observations, the pyrolysis process can be divided into five stages described by the following:

1. Warming up stage: In this first stage, normally no tangible bio-oil is produced and no visible gas can be observed at the outlet of the condenser. Generally, this stage ranges from 298.15 K up to approximately 550 K (Fig. 4). The term "warming up" is chosen to describe this stage because energy from the furnace is used to raise the temperature of the bed itself and part of the heat is being used to vaporise the moisture content of the biomass.
2. Mist stage: By increasing the temperature of the system above 550 K (Fig. 4), cracking of biomass starts. Experimentally, a light white mist can be observed at the outlet of the condenser and an odour is emitted as a result of the chemical reactions within the reactor. In this stage, the main portion of bio-oil production occurs in the reactor up to temperatures close to 781 K.
3. Cloud stage: Above 781 K, the mist thickens into a cloudy white outlet (Fig. 4). The odour of the outlet gas (both condensable and non-condensable gases) increases dramatically. Although the chemical reactions are faster in this temperature region between 781 K and 800.15 K, this stage only contributes below 10% of bio-oil production.
4. Yellow stage: When the cloud stage reaches a peak point, the outlet gas turns yellowish and finally, a thick yellowish brown colour is observed at the condenser outlet. Before this stage, the temperature reaches 800.15 K (targeted reaction temperature) in the bed. The chemical composition of the yellowish brown outlet gas requires further investigation which was beyond the scope of this study. In this stage, the outlet gas cannot be trapped in the condenser and the slight weight loss shown by the TGA curve occurs within the bed only. Generally, no noticeable increase in bio-oil production is obtained in the yellow stage.

5. Release stage: Finally, when all the biomass in the reactor is cracked into volatiles and only char remains, the pyrolysis process stops slowly. The outlet gas become visibly thinner and its colour changes first to white and then becomes invisible. The plateau at the end of the TGA curve in Fig. 4 indicates that no more volatiles are being produced. At the end of this stage, there will be no more gas exiting either the reactor or the condenser except for N_2 from the N_2 supply tank. The experimental run is then considered as finished.

The TGA curve in Fig. 4 also shows that over 90% of volatiles separation occurs during the highlighted region (A1) hence the area A1 corresponds to the main energy required to break the chemical bonds within the biomass and separate the volatiles with the target of producing bio-oil.

During the experimental runs, a sudden increase in temperature of the outlet volatiles prior to entering the condenser is observed especially in the Mist and Cloud stages. Although the pyrolysis process is generally considered as an endothermic process, partial exothermic processes are taking place while the main cracking process is proceeding. The results from the TGA/DSC unit confirms this as just after the Mist stage, the DSC curve has a low negative gradient which dramatically dives at the beginning of the Yellow stage before the end of the pyrolysis process.

3.6.1. Energy balance

In the experimental rig used, the energy consumption is higher compared to typical commercial production lines, but an energy balance for the designed unit can give an indication of the viability of the whole process when it is analysed realistically. This aim can only be achieved with the combination of the TGA/DSC results and the actual test rig results.

By integrating the power curve ($P(t)$) in Fig. 4 (dashed DSC curve), the thermal energy (E_{th}) required for the pyrolysis process (area A1) can be calculated using Eq. (17) as follows:

$$\int_{t_1}^{t_2} P(t)dt = \int_{t_1}^{t_2} \frac{dE_{th}}{dt} dt = E_{th} \tag{17}$$

This integration can be executed by using two different approaches:

(1) By curve fitting first and after finding the curve equation(s), the amount of energy can be determined by carrying out analytical integration. The accuracy of this method depends on the accuracy of the curve fitting method used.
(2) By applying trapezoidal rule (or other similar methods) in numerical integration, the amount of energy can be calculated by calculating the area A1 in Fig. 4. The accuracy of this method depends on the number of steps that is used to divide the area A1 in Fig. 4.

By using Eq. (17) and Fig. 4, the energy (area A1) required for cracking 11.23 mg of sample is calculated from the second approach to be 43.89 J (equivalent to 3.91 MJ for 1 kg of biomass). The yield of bio-oil at this experimental point is 50.08%. Therefore, the total energy consumption for the production of 1 kg bio-oil can be determined as follows:

$$E_{th} = 3.91 \times \frac{100}{50.08} = 7.81 \text{ MJ} \tag{18}$$

The gross calorific value of bio-oil measured at the same test point is 15.12 MJ/kg. This is 93.60% more than the input heating energy. This is not taking into account the remaining gaseous volatiles and char. The char (at same testing point), for instance, has a gross calorific value of 24.18 MJ/kg. Both the gas and solid remaining have the potential to be utilised as fuel, but this aspect falls beyond the scope of this study and is worthy of future investigation.

In Fig. 4, the summation of areas A1 and A2 (integration of solid DSC curve) represents the energy that is required to heat up the system until it reaches the targeted reaction temperature and maintain the system at the same temperature for the same length of time needed to crack 11.23 mg of sample. The combined area is 31% bigger compared to area A1 alone, which as explained previously represents the energy required to crack 11.23 mg sample in the TGA/DSC unit. This significant increase indicates that when cracking is initiated within the reactor, the exothermic reactions release a significant amount of heat into the system (especially during the Mist and Cloud stages). This additional heat helps the electrical furnace in further cracking the rest of the biomass, propagating like a chain reaction. The observations also imply that the more biomass there is in the reactor, the less the electrical energy from the furnace is required to crack the biomass. The major electrical energy of furnace is used to heat up the reactor walls itself. Therefore, it can be deduced that operating any pyrolysis unit at its full capacity (maximum possible biomass in reactor) aids in saving energy because the existing exothermic reactions help to develop the biomass cracking process.

4. Conclusions

The experimental results from a fixed-bed pyrolysis rig as well as the developed empirical correlations show that both reaction temperature and N_2 velocity strongly influence the yield and specifications of bio-oil produced from *J. curcas* pressed cake. At optimum pyrolysis conditions, above 50% of the waste is cracked down into bio-oil, which has less than 30% water content, a gross calorific value of 15.12 MJ/kg and a pH of 6.77. These properties demonstrate that the bio-oil can be used in burners without any modifications, if the rest of its specifications match that of the ASTM D7554-10 bio-fuel standard.

Acknowledgements

This work was supported by the Ministry of Agriculture, Malaysia under the Science Fund 05-02-12-SF1004. The Faculty of Engineering at the University of Nottingham Malaysia Campus is also acknowledged for its support towards this project. The authors would also like to thank the Bionas Group (Malaysia) for providing the *J. curcas* waste. Last but not least, the authors would like to thank Dr. Carol Eastwick and her team at the University of Nottingham, UK for their help in sample characterisation.

References

[1] Yaman S. Pyrolysis of biomass to produce fuels and chemical feedstocks. Energy Convers Manage 2004;45:651–71.
[2] Zhang Q, Chang J, Wang T, Xu Y. Review of biomass pyrolysis oil properties and upgrading research. Energy Convers Manage 2007;48:87–92.
[3] Balat M, Demirbas MF. Bio-oil from pyrolysis of black alder wood. Energy Source 2009;31A:1719–27.
[4] Mohan D, Pittman Jr CU, Steele PH. Pyrolysis of wood/biomass for bio-oil: a critical review. Energy Fuel 2006;20:848–89.
[5] Kumar S, Prakash R, Murugan S, Singh RK. Performance and emission analysis of blends of waste plastic oil obtained by catalytic pyrolysis of waste HDPE with diesel in a CI engine. Energy Convers Manage 2013;74:323–31.
[6] Pütün AE, Uzun BB, Apaydın E, Pütün E. Bio-oil from olive oil industry wastes: pyrolysis of olive residue under different conditions. Fuel Process Technol 2005;87:25–32.
[7] Oliveira JS, Leite PM, Souza LB, Mello VM, Silva EC, Rubim JC, et al. Characteristics and composition of *Jatropha gossypiifolia* and *Jatropha curcas* L. oils and application for biodiesel production. Biomass Bioenergy 2009;33:449–53.

[8] Singh RN, Vyas DK, Srivastava NSL, Narra M. SPRERI experience on holistic approach to utilize all parts of *Jatropha curcas* fruit for energy. Renew Energy 2009;33:1868–73.
[9] Vyas DK, Singh RN. Feasibility study of *Jatropha* seed husk as an open core gasifier feedstock. Renew Energy 2007;32:512–7.
[10] Manurung R, Wever DAZ, Wildschut J, Venderbosch RH, Hidayat H, Dam EG, et al. Valorisation of *Jatropha curcas* L. plant parts: Nut shell conversion to fast pyrolysis oil. Food Bioprod Process 2009;87:187–96.
[11] Sricharoenchaikul V, Atong D. Thermal decomposition study on *Jatropha curcas* L. waste using TGA and fixed bed reactor. J Anal Appl Pyrol 2009;85:155–62.
[12] Antony Raja S, Robert Kennedy Z, Pillai BC, Lindon Robert Lee C. Flash pyrolysis of *Jatropha* oil cake in electrically heated fluidized bed reactor. Energy 2010;35:2819–23.
[13] Sluiter A, Hames B, Hyman D, Payne C, Ruiz R, Scarlata C, et al., Determination of total solids in biomass and total dissolved solids in liquid process samples. National Renewable Energy Laboratory. NREL/TP-510-42621l; 2008.
[14] Darmstadt H, Garcia-Perez M, Adnot A, Chaala A, Kretschmer D, Roy C. Corrosion of metals by bio-oil obtained by vacuum pyrolysis of softwood bark residues: an X-ray photoelectron spectroscopy and auger electron spectroscopy study. Energy Fuels 2004;18:1291–301.
[15] Demirbas A. Pyrolysis of ground beech wood in irregular heating rate conditions. J Anal Appl Pyrol 2005;73:39–43.
[16] Elliott DC. Water, alkali and char in flash pyrolysis oils. Biomass Bioenergy 1994;7:179–85.
[17] Luo Z, Wang S, Liao Y, Zhou J, Gu Y, Cen K. Research on biomass fast pyrolysis for liquid fuel. Biomass Bioenergy 2004;26:455–62.
[18] Pütün AE, Apaydın E, Pütün E. Rice straw as a bio-oil source via pyrolysis and steam pyrolysis. Energy 2004;29:2171–80.
[19] Oasmaa A, Peacocke C. Properties and fuel use of biomass-derived fast pyrolysis liquids, a guide. VTT Journal. Publication number 731; 2010.
[20] Oasmaa A, Elliott DC, Muller S. Quality control in fast pyrolysis bio-oil production and use. Environ Prog Sustain Energy 2009;28:404–9.
[21] Malaysian Meteorology Department. Meteorology Metadata station page; 2013. <http://www.met.gov.my> [accessed 04.02.13].
[22] Salehi E, Abedi J, Harding T. Bio-oil from sawdust: pyrolysis of sawdust in a fixed-bed system. Energy Fuel 2007;23:3767–72.
[23] American Society for Testing and Materials. Standard specification for pyrolysis liquid biofuel. ASTM D7544-10; 2009.
[24] Spiegel MR, Stephens LJ. Multiple and partial correlation. Statistics. 3rd ed. Schum's outlines. Mc Graw-Hill; 1999.